A normal-incidence PtSi photoemissive detector with black silicon light-trapping

Martin Steglich, Matthias Zilk, Astrid Bingel, Christian Patzig, Thomas Käsebier, Frank Schrempel, Ernst-Bernhard Kley, and Andreas Tünnermann

Citation: Journal of Applied Physics **114**, 183102 (2013); doi: 10.1063/1.4829897
View online: http://dx.doi.org/10.1063/1.4829897
View Table of Contents: http://scitation.aip.org/content/aip/journal/jap/114/18?ver=pdfcov
Published by the AIP Publishing

A normal-incidence PtSi photoemissive detector with black silicon light-trapping

Martin Steglich,[1] Matthias Zilk,[1] Astrid Bingel,[1,2] Christian Patzig,[3] Thomas Käsebier,[1] Frank Schrempel,[1] Ernst-Bernhard Kley,[1,2] and Andreas Tünnermann[1,2]
[1]*Institute of Applied Physics, Abbe Center of Photonics, Friedrich Schiller University, Jena, Germany*
[2]*Fraunhofer Institute for Applied Optics and Precision Engineering IOF, Jena, Germany*
[3]*Fraunhofer Institute for Mechanics of Materials IWM, Halle, Germany*

(Received 6 August 2013; accepted 24 October 2013; published online 12 November 2013)

A normal-incidence light-trapping scheme relying on black silicon surface nanostructures for Si-based photoemissive detectors, operating in the IR spectral range, is proposed. An absorptance enhancement by a factor of 2–3 is demonstrated for technologically most relevant, ultrathin (2 nm–3 nm) PtSi rear layers on Si. It is shown that this increase can be translated into an equivalent increase in responsivity because of the absorption limitation of detector performance. Pd_2Si/p-Si detectors with black silicon are suggested as promising candidates for room temperature detection in the third optical window with an expected external quantum efficiency in the range of 9%–14%. © *2013 AIP Publishing LLC*. [http://dx.doi.org/10.1063/1.4829897]

INTRODUCTION

Silicon-based detectors for the infrared spectral region are of great importance because of their excellent reproducibility and low cost potential.[1] Since the intrinsic silicon absorption vanishes for sub-bandgap photons, Si detectors for $\lambda > 1100$ nm require more sophisticated concepts. A widely spread and relatively mature approach is to make use of the metal's light absorption in a Schottky diode. These detectors are known as *Schottky barrier photodiodes* or *photoemissive detectors*. Here, absorption of a photon generates a "hot" carrier which might overcome the Schottky barrier and, hence, be emitted into the silicon. Generally, the emission probability depends on the barrier height, the energy of the absorbed photon, and the mean distance a hot carrier can travel during its lifetime, which can also be understood as its attenuation length.[1] In addition to that, elastic hot carrier scattering at the metal interfaces leads to a drastic increase in emission probability if the metal film is very thin: Due to the statistical redirection of the carrier's momentum during the elastic interface scattering event, the chance rises that a carrier has a momentum sufficient to overcome the barrier.[2–5] This imposes an inherent trade-off between improving the internal quantum efficiency of the detector and the absorptance of the metal film. As a consequence, the best photoemissive detectors are fabricated with metal film thicknesses around only 2 nm.[6] Since these are semitransparent, efforts like waveguide integration of such detectors have been made lately to increase the absorptance and simultaneously keep the film thin.[7–9] In this publication, we propose the application of needle-like "black silicon" nanostructures for improved light-trapping and absorptance for normal-incidence radiation. This concept has the advantage of being highly compatible with existing manufacturing methods since illumination in photoemissive detectors occurs typically from the Si substrate side for improved refractive index matching. As an example, the most prominent PtSi/p-Si system will be examined in the following. On the basis of this particular detector class, this paper intends to demonstrate how existing Si photoemissive detectors can be improved by black silicon light-trapping and develop prospects how this concept enables sufficient detector performance for detection in the third optical window (around 1500 nm) at room temperature.

EXPERIMENTAL

Black silicon (b-Si) is a silicon surface nanostructure of statistically arranged Si needles or mountain-range-like features. In this work, they were prepared by inductively coupled plasma reactive ion etching (ICP-RIE) of Si wafers in an atmosphere of SF_6:O_2 = 1:1 at pressures of 1 Pa (deep b-Si) and 4 Pa (shallow b-Si). No chemical pre-treatment or (lithographic) masking of the wafers is necessary.[11,12] In addition, black silicon fabricated by ICP-RIE can be formed selectively using standard masking materials like photoresists or SiO_2 and effectively passivated by ultrathin Al_2O_3 layers.[10]

PtSi layers were fabricated by dynamic DC magnetron sputtering of Pt on Si and subsequent vacuum silicidation at about 350 °C for 5 min.[14] Prior to the Pt deposition, the Si substrates (double-side polished, [100] cut, 1–10 Ω cm, p-type, 525 μm thick) were cleaned by *in situ* Ar plasma etching. Layers of varying thicknesses were deposited on the polished rear sides of substrates with three different front surfaces: Shallow b-Si, deep b-Si, and as-polished. To preserve the comparability between all samples, the depositions were performed in one run per Pt thickness, and the silicidation conditions were kept identically.

Hemispherical reflectance (R) and transmittance (T) spectra were measured in a PerkinElmer 950 spectrometer with an integrating sphere. The samples were mounted with the polished Si or b-Si sides facing the incident light beam, respectively. To obtain an accurate complex refractive index of the fabricated PtSi layers, theoretical spectra were fitted to the measured spectra of the double-side polished samples.

For that purpose, the commercial software *SpectraRay* by Sentech Instruments was used. The refractive index of PtSi was modeled by a Drude-Lorentz oscillator dispersion model (ε, dielectric constant; ω, frequency; A, ω_0, β, const.)

$$\varepsilon = 1 + \frac{A}{\omega_0^2 - \omega^2 - i\beta\omega}. \quad (1)$$

For one sample, the PtSi film thickness was controlled by high resolution (scanning) transmission electron microscopy [HR-(S)TEM] analysis, in combination with energy-dispersive X-ray spectroscopy (STEM-EDXS), using an aberration-corrected *TITAN*^{3} *G2* 80-300 transmission electron microscope, equipped with a *SuperX*-EDXS detector (FEI company), operated at 300 kV.

Cross-sectional TEM samples were prepared following the standard procedure consisting of face-to-face gluing, embedding into alumina tubes, cutting, plane-parallel grinding and polishing, one-sided dimpling, both-sided Ar^+-beam etching at 2.5 keV under an incidence angle of 5°, and selective carbon coating.[13] Prior to preparation, a thin Cr protection layer was sputter deposited on top of the sample.

SIMULATION

Theoretical absorptance spectra of b-Si nanostructured samples with rear PtSi layers have been calculated using a hybrid method. Thereby the rigorous numerical solution of the scattering problem at the nanostructured interface was combined with an incoherent propagation scheme to treat the light propagation in the thick bulk region of the silicon wafer. In a first step the scattering response of both a periodic $5 \times 5\,\mu m^2$ patch of the b-Si surface and the plane rear side were calculated with the Fourier modal method.[15] The resulting amplitude scattering matrices that connect all incident and scattered diffraction orders at the interfaces were then converted into intensity based scattering matrices that resemble the Mueller calculus.[16] Finally, with the known Mueller scattering matrices the light propagation within the substrate was treated with an S-matrix algorithm[17] operating on incoherent Stokes vectors.[18]

For the PtSi rear layers the same complex refractive index data were assumed as obtained by previous modeling of the double-side polished samples. The silicon's optical constants were adapted from Ref. 19. Since this method is computationally highly demanding, we restricted the calculation to wavelengths in the range of 1250 nm–2500 nm. The obtained spectra exhibit several artificial kinks or oscillations. These arise from the sudden appearance and disappearance of propagating diffraction orders due to the periodic boundary conditions that were imposed to the finite lateral simulation area. To get reasonable spectra, these features were removed by moving average smoothing. Further information concerning the simulation method can be found in Ref. 18.

In order to estimate the internal quantum efficiencies of photoemissive PtSi/Si detectors, the thin-film single-barrier Schottky detector model by Scales and Berini was adopted.[20] In this phenomenological model, a hot electron in the metal will only overcome the Schottky barrier if its kinetic energy related to its momentum component perpendicular to the metal/silicon interface exceeds the barrier height Φ_B. In addition, it is assumed that the hot carrier's excess energy (above the Fermi level E_F) is purely kinetic. Then, the emission probability P over the barrier for a carrier with excess energy $E > \Phi_B$ can be written as

$$P(E) = \frac{1}{2}\left(1 - \sqrt{\frac{\Phi_B}{E}}\right). \quad (2)$$

An accurate description of the photoemission process also needs to take into account processes that lead to a decreased carrier excess energy. Multiple interactions will have such an effect, like scattering with phonons, impurities, defects, and cold carriers. In a simplified manner, all these processes can be considered in one single parameter, the hot carrier attenuation length L_n (or L_p for holes, respectively), which corresponds to the mean free path of the hot carrier before undergoing an scattering event. This is a rough simplification which can only be justified by using empirical values for $L_{n/p}$. Considering a huge number of hot carriers, the mean energy after traveling along the distance x can be estimated within this notion to be

$$E(x) = E_0 \exp(-x/L_{n/p}). \quad (3)$$

With hot carrier attenuation lengths in the range of tens of nanometers,[4,5,20,21] it can be advantageous to utilize a photoemissive metal layer which is much thinner than the hot carrier attenuation length. Then, in a ballistic roundtrip model, the hot carriers will undergo reflection at the rear dielectric/metal and the front metal/silicon interface if they are not emitted across the barrier. Assuming both reflection processes to be elastic and diffuse, this will greatly increase the overall emission probability. In this case, the total emission probability P^* can be written as

$$P^*(E_0) = \sum_{n=0}^{n_{\max}} P_n \prod_{k=0}^{n-1}(1 - P_k) \quad (4)$$

with (t, metal thickness, $h\nu$, photon energy)

$$n_{\max} = \frac{L}{2t}\ln\left(\frac{h\nu}{\Phi_B}\right), \quad (5)$$

$$P_k = P(E_k) = P\left[E_0 \exp\left(-\frac{2kt}{L_{n/p}}\right)\right]. \quad (6)$$

Finally, the internal quantum efficiency (*IQE*) for incident light of energy $h\nu$ can be calculated by integrating over a box type density of electron states $g(E) = const.$

$$IQE = \frac{\int_{\Phi_B}^{h\nu} g(E_0)P^*(E_0)dE_0}{\int_0^{h\nu} g(E_0)dE_0} = \frac{\int_{\Phi_B}^{h\nu} P^*(E_0)dE_0}{h\nu}. \quad (7)$$

The outlined calculation procedure is solved numerically. As shown by Scales and Berini,[20] it gives remarkably good results if the hot carrier attenuation length $L_{n/p}$ is treated as a fitting parameter. For the PtSi/Si detectors fabricated by Elabd and Kosonocky,[6] they obtained values of 150 nm and 56 nm for PtSi layers of thickness 3 nm and 8 nm, respectively. In this work, unless otherwise noted, a not too high value of $L_p = 80$ nm was assumed for hole emission and a barrier height Φ_B of 0.254 eV (Ref. 22) in the PtSi/Si(p) system. It should be noted that the latter represents an ideal value which is obtained as difference of the silicon's bandgap and the highest barrier value reported on n-Si. This would not hold if the barrier height is reduced by the presence of interface states or by image-force lowering,[22] which would give rise to a slightly raised cut-off wavelength and *IQE*, respectively. However, since silicide/silicon contacts are usually formed beneath the original silicon surface by heat treatment of deposited metal films, they are typically defect-free and, thus, show nearly ideal characteristics.[1,23]

Dark current density $j_{dark} = A^{**}T^2 \exp(-e\Phi_B/(kT))$ is calculated with the effective Richardson constant $A^{**} = 32\ \mathrm{A/(cm^2\ K^2)}$ for holes, according to Crowell and Sze.[22,24]

RESULTS

Theoretical predictions of the absorption behavior of ultrathin, semitransparent metal layers require precise knowledge of the layer's refractive index. For that purpose, Pt layers of varying thickness were sputtered on double-side polished Si wafers and silicided thereafter. The desired Pt thicknesses were estimated by assuming a constant deposition rate, as obtained from profilometry at thicker samples. In case of the 2 thinnest layers, a linear DC power-deposition rate relationship was furthermore expected. Under these assumptions, the deposited Pt layers are expected to be 1, 2, 5, and 10 nm thick, resulting in PtSi layers of about twice the thickness (i.e., 2, 4, 10, 20 nm).[1] Refractive indices of these layers in the range 1000–2500 nm were determined by fitting measured sample reflectance and transmittance spectra using a Drude-Lorentz oscillator model. Thereby, also the layers' thicknesses have to be used as fitting parameters since already slight variations in these have a huge impact on the fit results. As starting parameters the estimated values of 2, 4, 10, and 20 nm have been used. In order to ensure consistency of the results, it was implied that all layers have the same complex refractive index. In this spirit, all 8 reflectance and transmittance spectra of the samples were fitted at the same time, taking into account different layer thicknesses and allowing for variation of the latter. Figure 1 displays the fitting results. For clarity, here the absorptance spectra ($A = 1 - R - T$) are plotted instead of all R and T spectra. The typical fit's deviation from the R and T measurements is approximately the same in the depicted graphs. The agreement to the measurement is fairly good. Yet partially the fitted layer thicknesses deviate from the estimations significantly, especially in case of the thinner samples which are seen to tend to higher values. However, with regard to the changed deposition conditions (lowered DC power during deposition of the 2 thinnest samples) and the markedly short deposition durations of only a few seconds, these variations are hardly surprising and, thus, supposed to be real. To confirm the propriety of the fitting procedure used to determine the thin film thicknesses, the sample with the smallest PtSi film thickness was further analyzed by means of (scanning) TEM and EDXS analysis. As can be seen in Figure 1, the layer thickness of the thinnest PtSi layer (2.8 nm) that was obtained using the fitting procedure as described above can be assumed to be correct, within the limits of error due to sample preparation restraints and the fact that TEM gives highly localized information, in contradiction to the ellipsometry results that integrate over a rather large sample surface area. Therefore, it seems justified to calculate the thicknesses of all samples with a routine as described above.

The matter of fact that the obtained refractive index (Figure 1), when thickness deviations are allowed, is comparable to the one published by Mooney[25] supports this interpretation.

Like mentioned before, the technologically most interesting layer is the thinnest layer of only 2.8 nm thickness because of its inherently highest internal quantum efficiency η_i. However, the film's absorptance is the lowest, amounting to only ~13%.

To raise this small absorptance, our attempt is to apply black silicon nanostructures to the illumination facing silicon side of the detector. Such nanostructures have two positive optical effects. First, they act as an antireflection coating, which can be intelligibly understood in terms of an effective medium index gradient layer.[26] Second, they lead to a strong forward scattering of the incident light into higher angles of propagation such that the effective path length of light through the PtSi absorber layer is raised. The latter even yields the probability of strong light-trapping in the Si/PtSi device due to raised internal reflectance (or even total internal reflectance).[18]

In this work, two different black silicon nanostructures were examined. While the first has rather shallow feature depths of about 500 nm and small feature distances, the second exhibits greater depths of about 1700 nm and slightly larger feature distances (Figure 2). From our previous experiences with the optical behavior of those nanostructures, we expected the deeper structure to yield a stronger absorptance enhancement since it leads to a stronger forward scattering of incident light into higher angles and hence in an improved light-trapping.[27,28] It can be seen from Figure 3 that this anticipation is indeed correct. While both structures lead to a strongly increased absorptance, the effect of the deeper b-Si is even more pronounced. In particular, in the case of the thinnest PtSi film, the absorptance is raised by a factor of 4 to about 50% up to a wavelength of 2000 nm by this structure. The fair agreement between the simulated and the experimental spectra should also be noted. Although the calculations deviate measurably for the thin PtSi layers, the principle tendencies—the spectrum shapes, the thickness dependency, and the higher absorptance for the deeper nanostructures—are met. As an example, Figure 4 illustrates this for a fixed wavelength of 1550 nm, being important for telecommunication. The experimental and the calculated data are in good accordance, especially for the thicker films.

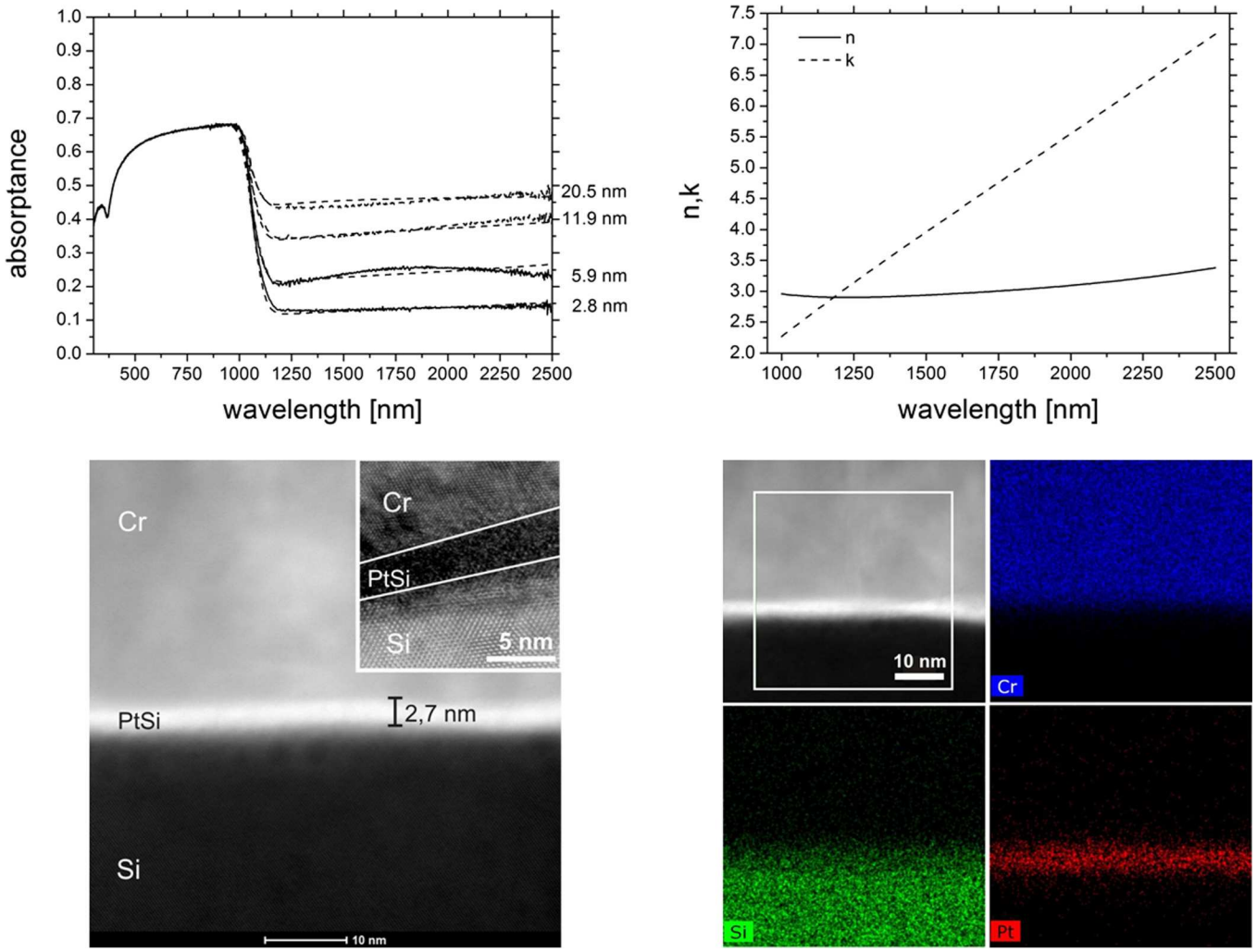

FIG. 1. Measured (straight lines) and calculated (dashed lines) absorptance spectra of the 4 PtSi layers on Si (top left). The graph also gives the corrected layer thicknesses, as obtained from the fitting procedure. For calculation, the fitted complex refractive index has been used (top right). Bottom left: STEM micrograph of a cross-sectioned sample with minimum PtSi thickness (interface area Si-PtSi-Cr). The inset shows a high-resolution TEM micrograph of the same sample. Bottom right: STEM micrograph (upper right panel, white frame highlights EDXS analysis area) and EDXS mappings of Cr, Si, and Pt of the same sample. The EDXS mappings confirm that the layer of bright contrast in the STEM micrograph is the PtSi layer.

Hence, we conclude that this confirms the validity of the conducted calculations and proves the applicability of our numerical method for first principle studies of different metal/Si photoemissive detectors with b-Si light-trapping structures.

A realistic prediction of achievable detector performance requires knowledge of the thickness dependent *IQE*. For that, we use the model by Scales and Berini.[20] As outlined above, it only requires the PtSi thickness, the Schottky barrier height Φ_B, and the free carrier attenuation length L_p

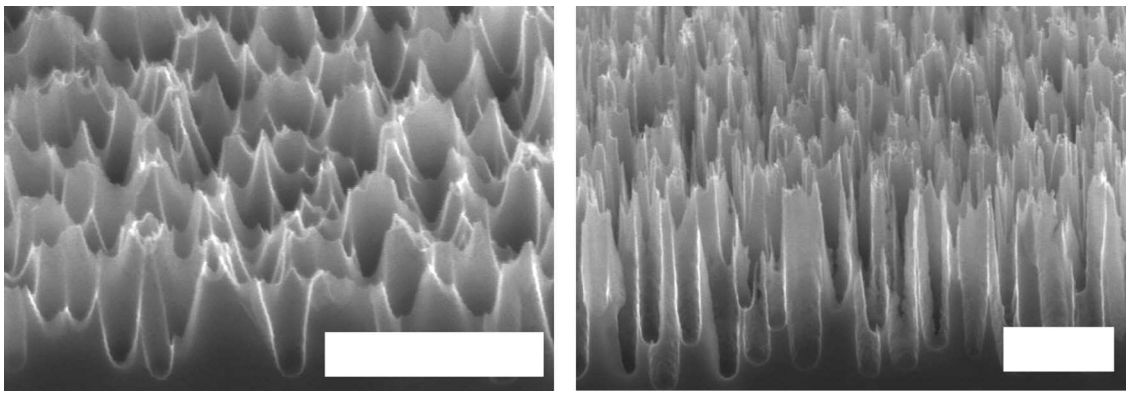

FIG. 2. Scanning electron images of the utilized shallow (left) and deep (right) black silicon nanostructures. The scale bar has a length of 1 μm. Note the different scaling.

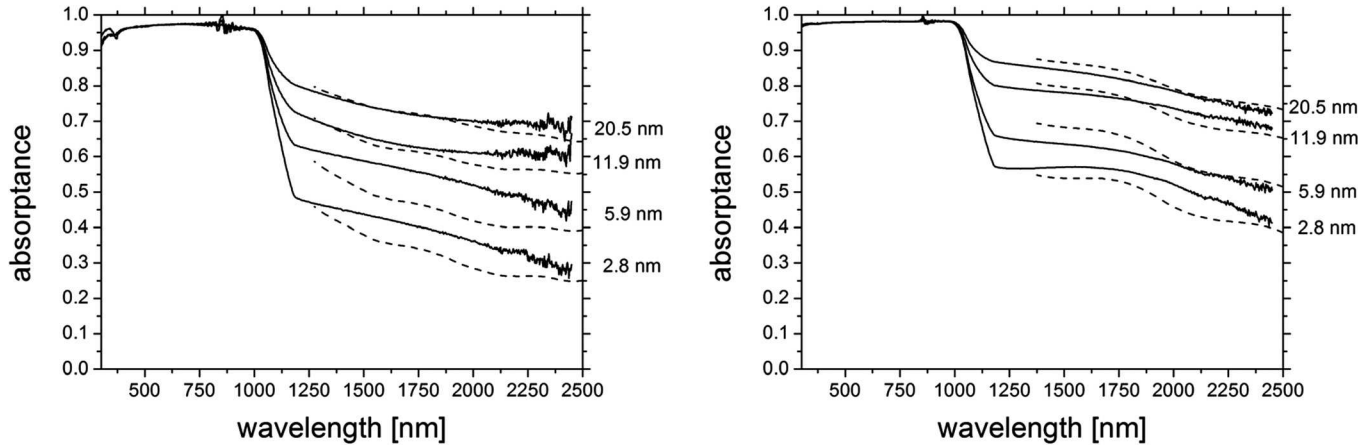

FIG. 3. Measured (straight lines) and calculated (dashed lines) absorptance spectra of the PtSi layers on the rear side of silicon wafers with shallow (left) and deep (right) black silicon nanostructure. The respective PtSi thickness is given next to the spectra.

as input parameters. To assure a conservative estimation of the *IQE*, only 80 nm was assumed for the latter whereas values of up to 150 nm are reported in the literature.[20] Figure 5 displays the resulting internal quantum efficiency at 1550 nm for the PtSi/p-Si detector with varying silicide thickness. In addition, also the (theoretical) absorptance *A* and the external quantum efficiency $EQE = IQE \times A$ for a detector with deep black silicon are plotted. While *A* grows with thickness, *IQE* decreases because of the vanishing effect of carrier reflection at the interfaces. As a consequence, a distinct optimum of about 20% is observable for the *EQE* around a layer thickness of 3 nm. This means that we can expect our 2.8 nm thick PtSi layer to show the best performance. Figure 6 gives a comparison of the expected *EQE* in the case of b-Si light-trapping structures atop the device and in the case of a polished Si front surface. This comparison, however, fails to some extent because it does not reflect realistic devices. Common PtSi/Si detectors comprise an additional single layer antireflection coating (SLAC) and a SiO_2/Al rear mirror to absorb a larger fraction of the incident light. To account for this, we performed calculations using the software *Open Filters*[29] to find out what the effect of such optimized system is. First, it has to be noted that the SLAC can only be optimized for a relatively narrow wavelength range compared to the broadband antireflection capabilities of a black silicon nanostructure since the SLAC condition $d_{SLAC} = \lambda/(4n_{SLAC})$ can only be ideally met for one single wavelength. Here, we chose the design wavelength λ to be 1550 nm. From a purely optical point of view, it is the best to use SiN for the SLAC since its refractive index of about 2 is near the optimal value of $n_{SLAC} = (n_{air} \cdot n_{Si})^{1/2} \approx 1.9$ in the considered spectral range. Hence, the numerically optimized system has the structure Air/SiN (194 nm)/Si/PtSi (2.8 nm)/SiO_2 (280 nm)/Al (opaque thickness) and results in a raised absorptance of about 28% at 1550 nm.

On the other hand, the PtSi/Si detector with b-Si light-trapping would also benefit from a rear mirror since the 2.8 nm thick PtSi is semi-transparent, and some fraction of light is lost in transmittance. To estimate the degree of benefit, additional reflectance and transmittance spectra of the sample with deep b-Si and 2.8 nm PtSi were recorded, where the sample was illuminated from the polished, PtSi coated rear side. With these spectra and the approximation that the reflectivity of the PtSi/Air interface equals the reflectivity of the PtSi/SiO_2 interface (which holds since the refractive indices n_{Air} and n_{SiO2} are similar to each other with regard to the PtSi's refractive index), a formula for the approximate fraction of transmitted light, that is re-absorbed through

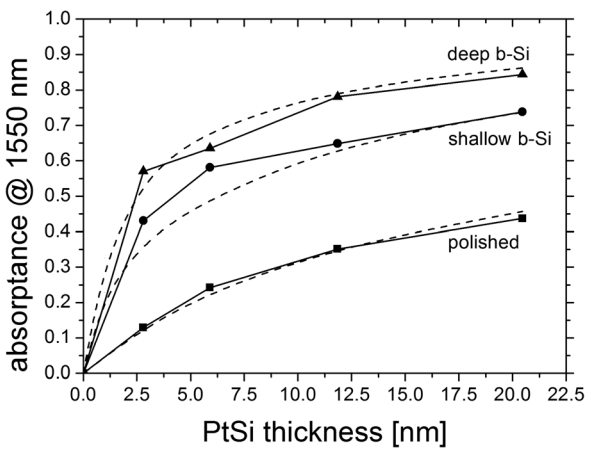

FIG. 4. Comparison of experimental (solid lines) and theoretical (dashed lines) absorptance at 1550 nm for different PtSi film thicknesses.

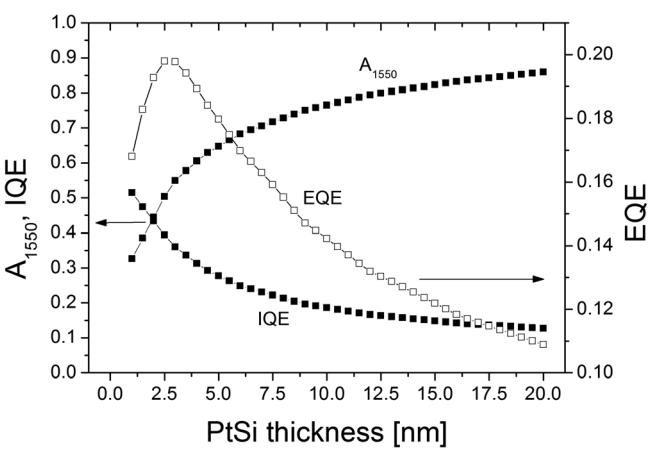

FIG. 5. Estimation of the optimum PtSi thickness in a PtSi/p-Si device with deep Black Silicon for detection at 1550 nm.

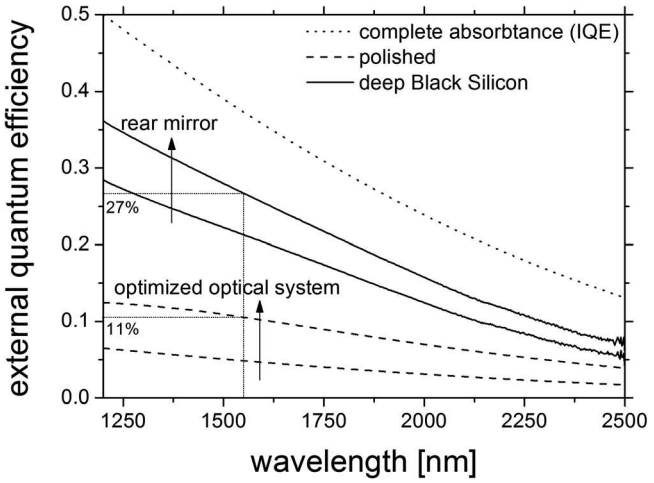

FIG. 6. Comparison of achievable external quantum efficiencies in normal-incidence PtSi/p-Si detectors with and without (deep) black silicon light-trapping. PtSi thickness is 2.8 nm. Optically optimized systems include a SiN-SLAC (only in the case of an unstructured, polished front surface) and a SiO_2/Al rear mirror for enhanced light absorption. The hypothetical curve for complete light absorption (corresponding to the IQE) is also shown.

application of the rear mirror, can be derived (A^*, R^*, measured absorbtance/reflectance under rear illumination; R_{Al}, finite Al mirror reflectance)[30]

$$f_{re-abs} \approx \frac{A^* R_{Al}}{1 - R^* R_{Al}}. \quad (8)$$

With that fraction of re-absorption f_{re-abs}, we can estimate the raised absorptance for the rear mirror enhanced detector with 2.8 nm PtSi and deep b-Si light-trapping. Using a realistic value of $R_{Al} = 0.975$, this estimation yields a f_{re-abs} that slowly decreases from 62% at 1200 nm to 30% at 2400 nm.

Both optimized detector systems—with and without b-Si light-trapping—are also included in Figure 6. The more realistic comparison between them yields, in principle, the same result like the comparison of the non-optimized structures: The absorptance and hence the *EQE* of the thin film PtSi/Si detector is raised by about a factor of 2 through the application of black silicon light-trapping. For instance, the EQE and responsivity $R\ [A/W] = EQE \cdot \lambda[\text{nm}]/1240$ reaches 27% and 0.33 A/W at 1550 nm compared to only 11% and 0.13 A/W in the optimized planar optical system with SiN-SLAC and Al rear mirror. A detector with black silicon and metallic rear mirror of 10 μm active diameter would have a dark current of about 120 μA at 300 K. Thus, for a 10 dB signal-to-noise ratio (SNR), a minimum detectable power of about 4 mW can be derived under the assumption of dominating dark current noise.

DISCUSSION

In 1985, Kosonocky *et al.* reported a PtSi/p-Si photoemissive detector with a PtSi thickness of 2 nm and about 18% *EQE* at 1650 nm, equipped with a SiO SLAC and a SiO/Al rear mirror for maximum light absorption.[31] Moreover, the authors noted a theoretical absorptance of ~30% at a design wavelength of 4 μm and a low barrier height Φ_B of 0.208 eV. Reconstructing and evaluating their optical cavity design with the refractive indices as obtained by us, we, however, end up with an absorptance of only 20% at 1650 nm. This means that an *IQE* of almost 100% is necessitated to obtain the reported 18% *EQE*. From the theoretical point of view, this is impossible. Thus, it is more reasonable to take into account several reasons for their surprisingly high *EQE*. First of all, the lower Schottky barrier of 0.208 eV—compared to the value of 0.254 eV supposed by us in this work—gives rise to a slightly higher *IQE*. Combining this with an increased hot carrier attenuation length of 150 nm (like in Ref. 20) results in a considerably improved *IQE* of about 60% at 1650 nm. Second, if we now speculate that 20% of absorptance is an underestimation of the PtSi film's real absorptance in Ref. 31, a high *EQE* of 18% seems feasible. However, since the refractive index data for PtSi as determined by us and by Mooney[25] differ only slightly at higher wavelengths (>2000 nm), an inaccurate optical calculation can be excluded from the list of possible sources of error. Another potential reason of absorptance underestimation is the PtSi layer's physical thickness. If, for example, the authors in Ref. 31 in fact had a slightly thicker PtSi film of 3 nm, the detector's absorptance would amount to ~30% and, in combination with 60% IQE, yield an EQE of 18% in the end. Interestingly, Scales and Berini drew a similar conclusion in their analysis of Kosonocky's data.[20] Checking Kosonocky's statement that the PtSi film had a thickness of one tenth of the skin depth at 4 μm, they also determined the thickness to be 3 nm rather than 2 nm.

Another comparison shall be made with the work by Chen *et al.*,[32] in which data for front-illuminated PtSi (2 nm)/p-Si detectors are presented. Relying on a rough estimation of the PtSi's refractive index, they derived an absorptance of 4.9% at 1500 nm and measured an *EQE* of 2.5%. However, from their measurements they also derived an *IQE* of 42% and hence a semi-theoretical *EQE* of only 2.1%. We think that this discrepancy between the measured and the calculated *EQE* in Ref. 32 can be explained by a slight underestimation of absorptance at 1500 nm. With our optical data, we obtain a higher absorptance of $A = 6.2\%$ for the detector configuration considered by Chen *et al*. Choosing $L_p = 80$ nm and $\Phi_B = 0.254$ eV like before, we get $IQE \approx 40\%$ at 1500 nm and hence an *EQE of* 2.5%, which is in excellent accordance to the experimental results in Ref. 32.

All together, we conclude that the presented results (i.e., the determined PtSi refractive index) in combination with the applied *IQE* calculation method are well suited to interpret the findings of other authors. Uncertainties, in particular, regarding the detector performance predictions that have been made, arise from differing published Schottky barrier heights. The second parameter which enters the calculation, the free carrier attenuation length L_p, reflects the electronic quality of the PtSi and typically ranges from 80 nm to 150 nm. Conservative estimates ($L_p = 80$ nm) reveal that the suggested b-Si light-trapping method may yield an *EQE* of 30% at 1500 nm. Disregarding the noted uncertainties in *IQE* calculation, any PtSi/Si detector (with given *IQE*) will be improved through the absorptance enhancement by a factor of 2 to 3 for relevant PtSi thicknesses between 2 nm and 3 nm.

We would like to emphasize that the presented black silicon light-trapping scheme is not restricted to the PtSi/Si

system. Clear benefits can be expected for other metal/Si (or silicide/Si) systems, too. Quantitative statements, however, always strongly depend on the utilized metal (silicide) and its complex refractive index. As an example, the Pd_2Si/p-Si system might be better suited for detection in the near-infrared at room-temperature because of its substantially higher Schottky barrier of 0.337 eV (Ref. 6) which, in turn, results in an about 20 times lower dark current. Assuming a film thickness of 2–3 nm and $L_p \approx 40$ nm, as determined in Ref. 20, we obtain an *IQE* of 15%–20% for this system. Since the optical function of Pd_2Si is similar to that of PtSi at 1550 nm,[33] we can assume a similar absorptance benefit by the b-Si nanostructure (i.e., $A = 60\%–70\%$) and hence get an *EQE* of 9%–14%. A hypothetical detector as before, with 10 μm active area diameter, would then have a dark current of 5 μA and, hence, a strongly reduced 10 dB minimum detectable power of 0.2–0.3 mW.

CONCLUSION

In this paper, we have demonstrated the beneficial effect of a black silicon light-trapping structure on the absorptance of ultra-thin rear PtSi films on Si both theoretically and experimentally. For that, the refractive index of PtSi has been determined and has been shown to be in good agreement with earlier data.[25] With these results, estimations of the achievable performance of photoemissive PtSi/p-Si detectors have been derived with the aid of a ballistic model for the carrier collection efficiency.[20] This model has been validated by applying it to literature data. Conservative estimates yield a feasible external quantum efficiency of about 30% at 1500 nm. As evidenced in the literature,[31] an even better device performance might be possible by the fabrication of higher quality PtSi layers.

Anyhow, by applying black silicon to the front surface an increase in efficiency by a factor of 2–3 can be achieved, compared to an optically optimized device with planar interfaces (utilizing an antireflection coating and a rear mirror).

Considering photoemissive Si detectors for the second and third optical window operating at room temperature, the combination Pd_2Si/p-Si is suggested rather than PtSi/p-Si. Evaluation gives an achievable external quantum efficiency of 9%–14% and a dark current of only 5 μA for a Pd_2Si/p-Si sensor with black silicon light-trapping and 10 μm active diameter at 300 K.

ACKNOWLEDGMENTS

The authors acknowledge the financial support by the ForMaT funding program of the German Federal Ministry of Education and Research under Contract No. 03FO3292. They also gratefully appreciate the fast and high-quality TEM sample preparation by A. Böbenroth (Fraunhofer IWM).

[1]A. Rogalski, *Infrared Detectors*, 2nd ed. (CRC Press, Boca Raton, 2011), p. 226.
[2]R. Taylor, L. Skolnik, B. Capone, W. Ewing, F. Shepherd, S. Rooshild, B. Cochrun, M. Cantella, J. Klein, and W. Kosonocky, "Improved platinum silicide IRCCD focal plane," Proc. SPIE **217**, 103–110 (1980).
[3]M. Kimata, M. Denda, T. Fukumoto, N. Tsubouchi, S. Uematsu, H. Shibata, T. Higuchi, T. Saeki, R. Tsunoda, and T. Kanno, "Platinum silicide Schottky-barrier IR-CCD image sensor," Jpn. J. Appl. Phys. **21**, 231–235 (1982).
[4]V. L. Dalal, "Simple model for internal photoemission," J. Appl. Phys. **42**(6), 2274–2279 (1971).
[5]V. E. Vickers, "Model of Schottky-barrier hot electron mode photodetection," Appl. Opt. **10**, 2190–2192 (1971).
[6]H. Elabd and W. F. Kosonocky, "Theory and measurements of photoresponse for thin film Pd2Si and PtSi infrared Schottky-barrier detectors with optical cavity," RCA Rev. **43**, 569–589 (1982).
[7]C. Scales, I. Breukelaar, R. Charbonneau, and P. Berini, "Infrared performance of symmetric surface-plasmon waveguide Schottky detectors in Si," J. Lightwave Technol. **29**(12), 1852–1860 (2011).
[8]S. Zhu, M. B. Yu, G. Q. Lo, and D. L. Kwong, "Near-infrared waveguide-based nickel silicide Schottky-barrier photodetector for optical communications," Appl. Phys. Lett. **92**, 081103 (2008).
[9]A. Akbari and P. Berini, "Schottky contact surface-plasmon detector integrated with an asymmetric metal stripe waveguide," Appl. Phys. Lett. **95**, 021104 (2009).
[10]M. Otto, M. Kroll, T. Käsebier, R. Salzer, A. Tünnermann, and R. B. Wehrspohn, "Extremely low surface recombination velocities in black silicon passivated by atomic layer deposition," Appl. Phys. Lett. **100**, 191603 (2012).
[11]H. Jansen, M. de Boer, R. Legtenberg, and M. Elwenspoek, "The black silicon method: a universal method for determining the parameter setting of a fluorine-based reactive ion etcher in deep silicon trench etching with profile control," J. Micromech. Microeng. **5**, 115–120 (1995).
[12]M. Steglich, T. Käsebier, I. Höger, K. Füchsel, A. Tünnermann, and E.-B. Kley, "Black silicon nanostructures on silicon thin films prepared by reactive ion etching," Chin. Opt. Lett. **11**, S10502 (2013).
[13]T. Höche, J. W. Gerlach, and T. Petsch, "Static-charging mitigation and contamination avoidance by selective carbon coating of TEM samples," Ultramicroscopy **106**, 981–985 (2006).
[14]G. Larrieu, E. Dubois, X. Wallart, X. Baie, and J. Katcki, "Formation of platinum-based silicide contacts: Kinetics, stoichiometry, and current drive capabilities," J. Appl. Phys. **94**(12), 7801–7810 (2003).
[15]L. Li, "New formulation of the Fourier modal method for crossed surface-relief gratings," J. Opt. Soc. Am. A **14**, 2758–2767 (1997).
[16]K. Kim, L. Mandel, and E. Wolf, "Relationship between Jones and Mueller matrices for random media," J. Opt. Soc. Am. A **4**, 433–437 (1987).
[17]L. Li, "Formulation and comparison of two recursive matrix algorithms for modeling layered diffraction gratings," J. Opt. Soc. Am. A **13**, 1024–1035 (1996).
[18]M. Kroll, M. Otto, T. Käsebier, K. Füchsel, R. Wehrspohn, E.-B. Kley, A. Tünnermann, and T. Pertsch, "Black silicon for solar cell applications," Proc. SPIE **8438**, 843817 (2012).
[19]M. A. Green, Sol. Energy Mater. Sol. Cells **92**, 1305 (2008).
[20]C. Scales and P. Berini, "Thin-film Schottky barrier photodetector models," IEEE J. Quantum Electron. **46**(5), 633–643 (2010).
[21]W. Pong, H. K. Nishihara, and D. Chan, "Effect of boundary scattering on photoemission from thin films," J. Opt. Soc. Am. **62**(4), 487–490 (1972).
[22]S. M. Sze and K. K. Ng, *Physics of Semiconductor Devices*, 3rd ed. (Wiley, New Jersey, 2007), p. 180.
[23]J. M. Andrews and M. P. Lepselter, "Reverse current-voltage characteristics of metal-silicide Schottky diodes," Solid State Electron. **13**, 1011 (1970).
[24]C. R. Crowell and S. M. Sze, "Quantum-mechanical reflection of electrons at metal-semiconductor barriers: Electron transport in semiconductor-metal-semiconductor structures," J. Appl. Phys. **37**, 2683 (1966).
[25]J. M. Mooney, "Infrared absorption of thin PtSi films between 1 and 6 μm," J. Appl. Phys. **64**, 4664 (1988).
[26]W. H. Southwell, "Pyramid-array surface-relief structures producing antireflection index matching on optical surfaces," J. Opt. Soc. Am. A **8**(3), 549–553 (1991).
[27]M. Steglich, M. Zilk, F. Schrempel, A. Tünnermann, and E.-B. Kley, "Improvement of Ge-on-Si photodiodes by black silicon light trapping," Appl. Phys. Lett. **102**, 111110 (2013).
[28]M. Kroll, T. Käsebier, M. Otto, R. Salzer, R. Wehrspohn, E.-B. Kley, A. Tünnermann, and T. Pertsch, "Optical modelling of needle-like silicon

surfaces produced by an ICP-RIE process," Proc. SPIE **7725**, 772505 (2010).
[29]S. Larouche and L. Martinu, "OpenFilters: open-source software for the design, optimization, and synthesis of optical filters," Appl. Opt. **47**(13), C219–C230 (2008).
[30]See supplementary material at http://dx.doi.org/10.1063/1.4829897 for a detailed derivation of the formula.
[31]W. F. Kosonocky, F. V. Shallcross, T. S. Villani, and J. V. Groppe, "160×244 element PtSi Schottky-barrier IR-CCD image sensor," IEEE Trans. Electron Devices **32**(8), 1564–1572 (1985).
[32]C. K. Chen, B. Nechay, and B.-Y. Tsaur, "Ultraviolet, visible, and infrared response of PtSi Schottky-barrier detectors operated in the front-illuminated mode," IEEE Trans. Electron Devices **38**(5), 1094–1103 (1991).
[33]See www.ioffe.ru/SVA/NSM/nk/ for IOFFE n&k database.